

Quantum key establishment via a multimode fiber

Lyubov V. Amitonova^{1,2,3,*}, Tristan B. H. Tentrup¹, Ivo M. Vellekoop² and Pepijn W. H. Pinkse¹

¹Complex Photonic Systems (COPS), MESA+ Institute for Nanotechnology, University of Twente, PO Box 217, 7500 AE Enschede, The Netherlands

²Biomedical Photonic Imaging, Technical Medical Centre, University of Twente, PO Box 217, 7500 AE Enschede, The Netherlands

³LaserLaB, Department of Physics and Astronomy, Vrije Universiteit Amsterdam, De Boelelaan 1081, 1081 HV Amsterdam, The Netherlands

*e-mail: l.amitonova@vu.nl

ABSTRACT

Quantum communication aims to provide absolutely secure transmission of secret information. State-of-the-art methods encode symbols into single photons or coherent light with much less than one photon on average. For long distance communication, typically a single-mode fiber is used and significant effort has been devoted already to increase the data carrying capacity of a single optical line. Here we propose and demonstrate a fundamentally new concept for high-dimensional remote key establishment. Our method uses a quantum-secure wavefront shaping procedure to transmit information through a light-scrambling multimode fiber. It detects eavesdropper attacks without using randomly switched mutually unbiased bases. Moreover, it sends information in a deterministic way, allowing direct decoding at the receiver end. We prove that it is secure with weak coherent light even when several photons per symbol are used. Given sufficient scrambling by the multimode fiber, our method relies on the no-cloning theorem only. Since it is optical fiber based, our method allows to naturally extend secure communication to larger distances. We experimentally demonstrated this new type of key exchange method by encoding information into a few-photon light pulse decomposed over guided modes of an easily available step-index multimode fiber.

INTRODUCTION

The importance of secure communication is rapidly growing¹. We use cryptography in everyday life often without noticing, for example, when we conduct financial transactions via the internet. The security of conventional cryptography is based on shared secret keys or on computational assumptions, such as the presumed hardness of factoring². In practice, this means that it is vulnerable to unanticipated advances in hardware or algorithms. Quantum cryptography in theory provides unconditional secure communication, assuming only that an eavesdropper (Eve) is restricted by the laws of physics: the quantum no-cloning theorem forbids to replicate an unknown quantum state³. Indeed, the security of quantum cryptography requires quantum states of light⁴. For example, in the original and best-known quantum key distribution (QKD) method – BB84 proposed by Bennett and Brassard⁵ – the security is based on the fact that the polarization of a single photon can be prepared and measured along well-defined directions. Key distribution methods do not by themselves communicate useful information, but such a communication can follow with the proven-secure one-time-pad method after the secure key is built up.

Nowadays, optical fibers are key elements of worldwide communication networks⁶. Single-mode fibers are widely used to transmit voice, television and internet data. The ultimate goal is to increase the data-carrying capacity of a single line. Combining multiple strands of fiber in a single optical cable enable various spatial division multiplexing schemes. This allows the merging of high-dimensional QKD systems with optical fiber transmission. Multicore fibers are also being studied for space-division multiplexing⁷ and have been used for high-dimensional QKD⁸. A step-index multimode (MM) fiber supports a significantly higher number of modes than a multicore fiber and as a result can transfer information at a higher density. Another method for secure communication relies on optical reciprocity in MM fibers scrambling wavefronts in a random way⁹.

Although short pieces of straight or slightly bent fiber are not truly random¹⁰, in any realistic fiber random bends, index imperfections, and other perturbations cause the signal to couple into multiple modes¹¹, leading to an arbitrary mixing of field amplitudes¹² and scrambling the information across the modes. However, it is well-known that the mode mixing can be partially undone by applying techniques from complex wavefront shaping, a method originally developed for precise light control through and in highly scattering materials^{13–15}. Recently methods have been proposed for high-speed¹⁶, high-resolution^{17,18} image transfer. Multimode optical fibers can now also be used to transmit information in the spatial domain^{19–21}. However, these methods are not secure.

Here we propose a new method for secure key establishment via a MM fiber. The idea is based on secure characterization of the multimode transmission channel by means of weak light pulses. As can be seen in Fig. 1, both the sender, Alice, and the receiver, Bob, control a stretch of fiber that is randomly bent so that it spatially scrambles the optical communication signal. Our method is designed such that:

- 1) Alice and Bob can characterize the scrambled communication channel in a calibration phase and undo the scrambling using complex wavefront shaping in the communication phase.
- 2) By merit of the no-cloning theorem, Eve cannot decode the signal without physically reproducing the exact configuration of the scramblers used by Alice and Bob.
- 3) By merit of the same theorem, Eve cannot determine the configurations of the scramblers, even when she is intercepting the optical signals in the calibration and/or communication phases. Since she doesn't know the configuration of the scramblers, by 2), she cannot decode the signal.
- 4) If Eve tries to hide her interception by resending light to Bob, this can easily be detected. We can quantify the amount of information that she can collect when tapping only a small portion of the signal.

Elements 1, 2 and 4 are sufficient to ensure secure key establishment in the case that Eve has no method to build a physical copy of the entire multimode communication channel. Element 3 ensures that our method remains secure in the case that Eve has access to some technology to clone or mimic exactly the stretches of distorted multimode fiber. Compared to traditional QKD, it can be noticed that our method doesn't require two mutual unbiased bases, which are conventionally used to detect Eve's attacks. It also doesn't need a quantum key sifting step, and the fiber nature of the proposed method allows to extend our method to long distances. Finally, our method does not require the light to be in an entangled (or otherwise special) quantum state; a weak coherent state suffices.

RESULTS

The method

Firstly, we briefly discuss the main idea of the method under ideal conditions assuming a perfect single-photon source and ideal wavefront shaping (in phase and amplitude), since this is the simplest to understand conceptually. In the Methods section we give a quantitative argument why the method is still secure with weak coherent light and imperfect wavefront shaping without any adaptation to the method or the setup. The experimental setup and illustration of the main principle are presented in Fig. 1. Alice and Bob each have under full control a short fragment of MM fiber, which act as a ‘scrambler’. They both ‘program’ the scrambler in a random way by applying a random conformational change to the fiber. In the calibration phase, Alice and Bob perform a stepwise sequential wavefront shaping algorithm^{22,23}: Alice generates a plane wave with a single segment that is phase shifted. Bob records a camera frame and sends it to Alice via a classical channel. This is repeated for each segment several times. After this calibration phase, Alice can now use wavefront shaping to focus light on any desired position on Bob’s camera. In this way, we can encode a high-dimensional alphabet into the guided modes of a multimode fiber. The set of special superpositions of fiber modes that lead to light focused at desired points on Bob’s side we will call a basis.

To send a symbol, Alice prepares a single-photon quantum state with an appropriately phase-shaped and amplitude-shaped wavefront that leads to a focus of light at the particular position on the fiber output facet. Throughout the fiber, the single photon will be present as a disordered superposition of almost all fiber modes. If a potential eavesdropper Eve would intercept the photon and determine its position, the photon collapses at a nearly random position on Eve’s detector, which varies even between identical copies of the same symbol (see Fig. 1 ‘Eve’). Therefore, Eve will not be able to identify what symbol was sent: the information is scrambled. Only at Bob’s end, the photon will be spatially localized at the target position, where each target position corresponds to a symbol from the alphabet (see Fig. 1 ‘Bob’). Since here the photon is spatially localized, Bob can unambiguously identify what symbol was sent: the information is *unlocked*.

As a result, Bob can decode the information instantaneously during the communication via multimode fiber. Under ideal conditions, no classical postprocessing is required. In case of nonperfect wavefront shaping and/or losses within the system, Bob reports to Alice which characters should be discarded from the final key, as a last step.

Experimental demonstration

We perform our experiments in imperfect ‘real-life’ conditions: with a weak coherent light source, in the presence of noise, and assuming only a moderate efficiency of wavefront shaping. First, the fiber is calibrated in its current configuration as described in the Materials and Methods section. In experiments, we use a fiber with an approximate number of 1500 modes ($N = 1500$, see the Materials and Methods section) and the alphanumeric: 36-dimensional alphabet consisting of A-Z + 0-9 (case insensitive) symbols. The symbols are encoded into 36 different positions on the fiber output facet, as presented in faint green circles in Fig. 2(a).

In the first set of experiments, we emulate the perfect single-photon source by taking into account only the frames with single-photon detection events. Snapshots of the spatial distributions of photons measured by Bob and by Eve are presented in Fig. 2(a) and 2(b), respectively. For clarity, we show frames which correspond to the fidelity of wavefront shaping $\alpha^2 = 0.6$ (for the definition of fidelity see the Materials and Methods section) and for only two different symbols sent by Alice by open and filled

dots. Different colors represent 10 different repetitions of each of the two symbols. The dashed line shows the fiber core edge. In contrast to Eve, Bob clearly sees the correlation between different realizations of the same symbol. In case of a perfect single-photon light source, the probability for Bob to detect the photon in the correct position is equal to the fidelity of wavefront shaping that, as was shown before, can experimentally reach a theoretical maximum of $\pi/4$ for phase-only wavefront shaping¹⁹. In contrast, different realizations of the same field pattern hardly correlate to each other on Eve's side (see Fig. 2(b)).

In the second set of experiments, we characterize the communication between Alice and Bob for low-fidelity wavefront shaping, $\alpha^2 = 0.1$, and assuming a weak coherent light source with an average number of photons per pulse \bar{n}_a starting from 2. Alice sends each of the 36 symbols 200 times in random order. Each time, Bob reads the signal on the fiber output and estimates what symbol was sent. Bob can use two main strategies. In the first strategy, Bob compares the number of photons in different predefined areas and chooses the one with the highest intensity. In the second strategy, Bob selects only those transmissions for which he is very sure what symbol was sent by accepting only the symbols with at least as many photons as a particular threshold. Whenever Bob has more information than Eve, the few-percent error rate can be corrected down to the standard 10^{-9} during the (classical) error correction step of the protocol²⁴.

We investigate the percentage of the correct reading and the rejection ratio for two different thresholds. Then we repeat the whole procedure for a different average number of photons per pulse. The results averaged over all 36 symbols are presented in Fig. 2(c), where the probability p to detect the correct symbol versus the average number of photons in a pulse, \bar{n}_a , is plotted for different strategies of Bob: black, no threshold; red, two-photon threshold and blue, three-photon threshold. Dots represent the experimentally measured data. The black line shows the theoretical prediction from the following formula $p = e^{-\lambda_1} \sum_{k=0}^{\infty} [F(k-1)]^{S-1} \lambda_1^k / k!$, where $F(k) = e^{-\lambda_2} \sum_{l=0}^k \lambda_2^l / l!$ is the cumulative distribution function of the Poisson distribution, λ_1 is the average number of photons at the “correct” position, λ_2 is the average number of photons at the “wrong” position, and S is the total number of symbols. Values $\lambda_1 = 0.1\bar{n}_a$ and $\lambda_2 = 0.005\bar{n}_a$ were extracted from the experimental data. The blue and red lines represent the results of simulations of Bob's probability for a threshold of 2 photons and 3 photons, respectively. Although even in the case of low fidelity of wavefront shaping ($\alpha^2 = 0.1$) and no threshold the probability of reading the correct answer is significant, it dramatically increases for strategies with a threshold. The rejection rates are also carefully analyzed and presented in Fig. 2(d) for a threshold of 2 photons (red bars) and 3 photons (blue bars). The width of the bars corresponds to the standard deviation of the number of photons in a pulse and increases according to the Poisson distribution. As a result, Bob can read information with an error rate close to zero.

Security analysis

Let us assume that the eavesdropper can tap off the signal somewhere in the middle of the fiber. Eve can only retrieve a fraction of the information that was sent by taking snapshots of the complex wavefronts in the fiber, since she cannot sort the wavefronts in S symbols in a passive linear way such as happens at Bob's fiber end. In the Materials and Methods section below, we derive a strict upper limit for the amount of information that Eve can gain in case of a *single-photon light source* as $\langle H_E \rangle = (1 - \gamma)/\ln 2 \approx 0.61$ bit per transmitted symbol regardless of the number of symbols or the number of modes, where γ is the Euler constant. Under the same conditions Bob at maximum can have $H_B = \log_2(S) \approx 5.2$ bit of

information per transmitted symbol for $S = 36$ symbols. As a result, $\langle H_E \rangle \ll H_B$, guaranteeing the security of the method.

If rather than single photons *weak coherent light is used*, phase measurements are possible. The fundamental limit of the best possible fidelity β^2 with which Eve can measure the wavefront with a low photon budget is determined by the following expression: $\beta^2 = \bar{n}_a / (\bar{n}_a + 2N)$, where \bar{n}_a is the average number of photons per pulse sent by Alice and N the number of fiber-guided modes²⁵. We calculate the amount of information per transmitted symbol that Eve can retrieve at best for $N = 1500$ fiber modes and $S = 36$ symbols. The results are present in Fig. 3(a) where the blue line represents the exact upper limit (evaluated through a numerical integration method, see the Materials and Methods section for the details) and the red line represents a simple closed-form analytical upper limit. We see that H_E is below the maximum entropy achievable by Bob ($\log_2 S$) even when the average number of photons exceeds one.

Note that we have to explicitly exclude the scenario where Eve knows part of the message, since in this case she could sum the measurements for corresponding symbols together, eventually collecting enough information. Therefore, our method is limited to distributing messages which appear completely random to Eve. Because of the unique properties of the method we introduce here, data is transferred in a deterministic manner, removing the necessity of a quantum key sifting step, allowing Bob to decode the information instantaneously during the communication. Although this allows to directly communicate secretly²⁶, there is always the risk of leaking a fraction of this information to Eve and we do not follow that route here and instead assume that our method is used to establish a secret key.

One may argue that Eve could, hypothetically, copy and physically reproduce all essential features of the fiber between Eve and Bob in some passive optical system that would focus each symbol onto a different detector. Constructing such a programmable mode sorter which implements any linear transmission matrix is theoretically possible, although it remains an extremely challenging technological problem^{27,28}. However, even with the ultimate technology, Eve cannot build a mode sorter without knowledge of the exact transmission matrix. Obviously, Eve cannot directly measure the transmission matrix of the scramblers of Alice and Bob because these parts of the fiber are always kept under the control of Alice and Bob. Therefore, we only have to make sure that Eve cannot find out the transmission matrix by intercepting the calibration phase and/or the communication phase.

To ensure that Eve cannot intercept the calibration phase, we made two small modifications to the stepwise sequential wavefront shaping algorithm. First of all, Alice sends the wavefronts in a random order, so that Eve does not know what pattern was sent. Second, Alice sends spatially shaped waves that only contain a single photon at a time. Since, again, this single photon will be present as a disordered superposition of almost all fiber modes, Eve has no way to find out what wavefront Alice has sent. Moreover, the no-cloning theorem forbids Eve to ‘replay’ the field to Bob’s fiber after doing a measurement. Therefore, she will have to send some arbitrary wavefront instead. After all measurements, Alice sums all corresponding frames for each measurement. She now has high-contrast speckle images that she can use to calculate the transmission matrix. Eve on the other hand, does not know what frames belong to what measurement, so she has no way to combine the frames into a high-quality image. In addition, if Eve intercepted the communication during the calibration phase, she will have sent arbitrary wavefronts to Bob, thereby breaking the correlation between Alice’s transmitted field and Bob’s response. As a result, when Alice now sums the corresponding frames, she will get low-contrast (uniformly distributed) images. This way, Alice can detect the presence of Eve without giving away any information.

DISCUSSION

In our experiments, the bit rate was limited by the speed of the camera. With high-speed cameras or avalanche photodiode arrays, the limitation of the proposed method might be the speed at which phase masks can be changed. The digital micromirror device (refresh rate up to 22 kHz) together with the high dimensionality of the used alphabet ($H_B = \log_2 36 = 5.2$ bit per pulse) gives rise to a secure bit rate of up to 0.12 Mb/s. The bit rate can be increased twofold without any changes in the setup and equipment by increasing the number of symbols²⁹. Further improvements can be made by increasing the number of guided modes of the multimode fiber. Commercially available multimode fibers support up to $3 \cdot 10^6$ modes, which is 2000 times more than we used in the present experiments. Such a fiber correspondingly allows to increase the dimensionality of the quantum channel and consequently the level of security.

To address the fundamental limit of the maximal fiber length that could be used in the proposed method of remote key establishment, we analyze pulse spreading within the multimode fiber. A high bit rate limits possible laser bandwidth and, as a result, its coherence length, which is of key importance for effective wavefront shaping procedure. We estimate that the fiber length can be more than 800 km for the maximal bit rate supported by the digital micromirror device and a standard MM fiber with NA of 0.22 (see Supplementary material of Ref. 20) before pulse spreading limits our method.

Further, we address the way how losses affect remote key establishment in the proposed approach. In principle, losses may leak information to the eavesdropper: for coherent pulses this is certainly the case; for single photons it is not⁴. In case of a *single-photon light source*, if a photon does not arrive, the detector does not click and the event is simply discarded.

Losses in case of a *weak coherent light source* will affect the security of a protocol. We analyzed the parameters (see the Materials and Methods section for the details) for which the amount of information gained by Bob under imperfect conditions is more than the theoretically possible maximum of information gained by Eve. If we assume that Bob has single-photon detection sensitivity, we can calculate the accessible losses of a system. The results are present in Fig. 3(b), showing the maximum tolerable losses in dB under which the method is still secure, plotted as a function of the wavefront shaping fidelity, α^2 and the number of modes, N for the number of symbols $S = 36$. We see that a high level of wavefront shaping fidelity together with relatively high number of modes (in comparison with the number of symbols) allow a fair amount of acceptable losses in case of a *weak coherent light source*. For the parameters of our experiment with fidelity $\alpha^2 = 0.1$ and $S = 36$ symbols, losses of 5.3 dB still guarantee the security of the protocol (see Fig. 3(b)). For a fiber with 200 μm core diameter and exactly the same parameters of the setup including low wavefront shaping fidelity, the tolerance to noise increases to up to 9 dB. The multimode fiber used in our experiments has minimal losses of 0.7 dB/km, according to the specification [Thorlabs]. As a result, our method already works with a weak coherent light source at more than 7 km distance, which can be easily upgraded.

To summarize, we propose and implement a new type of key exchange method that is secure by encoding information into a few-photon light pulse decomposed over guided modes of a multimode fiber. The new method is based on the no-cloning theorem combined with random light scrambling and secure wavefront shaping. The method guarantees the secure establishment of a shared key in case of a single-photon source, as well as in the case of a weak coherent light source with a low (relative to the number of modes) photon number. Moreover, it works with a high-dimensional alphabet, and can be naturally extended to larger distances.

MATERIALS AND METHODS

Experimental setup

Alice uses the continuous-wave linearly polarized output of a He-Ne laser with a wavelength of 633 nm (see Fig. 1 ‘Alice’). Neutral-density filters in combination with a half-wave plate and a polarizing beam splitter are used to reduce the power to the desired level. A single-mode fiber is used to clean the laser mode and to expand the laser beam in order to match the surface of a spatial light modulator. To control the spatial phase of the coupled light with high speed, Alice uses a 1920x1200 Vialux V4100 digital micromirror device (DMD). The lenses L_1 and L_2 are placed in a 4f-configuration to image the phase mask on the back focal plane of a coupling objective. A pinhole in the Fourier plane blocks all the diffraction orders except the 1st, which encodes the desired spatial phase distribution. An objective with NA = 0.4 (Olympus) is used to couple light into a conventional step-index multimode fiber (Thorlabs, FG050UGA) with a silica core of $d_c = 50 \mu\text{m}$ diameter and numerical aperture NA = 0.22. Such a fiber has a normalized frequency $V = \pi d_c \text{NA}/\lambda \approx 55$ for our laser wavelength, $\lambda = 633 \text{ nm}$, and sustains approximately $N = 1500$ guided modes¹². The part of the experimental setup described above belongs to Alice and potentially allows encoding the desired symbol with a speed of up to 22 kHz. The multimode fiber serves as a quantum channel to deliver symbols to Bob in such a way that anyone who wants to listen to the communication at any arbitrary position along the fiber fails. We mimic the situation when Eve has access to the fiber without Alice and Bob knowing so, dividing the quantum channel into two parts. Each piece of the multimode fiber is 3 meters long. Eve’s part of the setup includes two objectives (Olympus, NA = 0.4) served to close a gap between two pieces of fiber and to image the fiber output on her camera (see Fig. 1 ‘Eve’). Bob’s part of the setup includes one objective (Olympus, NA = 0.4) to image the fiber output on the camera (see Fig. 1 ‘Bob’). Bob and Eve use a high-sensitive intensified charge-coupled device (ICCD) camera to detect light at the single-photon level (see ‘Image processing’ section). Light will pass from Alice to Eve, where it is split at M2, from where a part falls on Eve’s camera and a part continues to Bob through the second fiber. During the calibration and characterization of Bob’s part we use the first pathway and during the characterization of Eve’s part we use the second pathway

Calibration and wavefront shaping procedure

The complex wavefront-shaping algorithm to create a focused laser spot on the fiber output facet without information about the configuration of the fiber-based scrambler is as follows. We use the DMD to control the spatial phase profile of light at the fiber output facet. Each mirror of the DMD can be set to two different tilt angles. By controlling the tilt of every mirror, 2D binary gratings can be created³⁰. With an appropriately tilted input light field, the diffracted light propagates along the normal of the DMD surface (see Fig. 1 ‘Alice’). The DMD area of 510×510 pixels covered by an expanded laser beam is divided into $N_{seg} = 34 \times 34$ segments. Each segment consists of 15×15 micromirrors. Alice modulates the phase of a single segment by shifting the grating pattern over 2π in three steps. In total 3468 different phase masks were used. To guarantee the security of the wavefront shaping procedure, each pulse Alice sends contains only 80 ± 30 photons. The single segment that is modified contains on average less than a photon. Bob measures the intensity in $S = 36$ points on the fiber output facet or on a camera frame and sends this information back to Alice via a classical channel. In our experiments, a grid of 6×6 points with $3.2 \mu\text{m}$ step size on the fiber output is used. However, the position of the symbols is not restricted and can be selected randomly. They repeat the measurements 50 times for each phase

mask in random order. After all measurements, Alice sums all corresponding frames for each measurement. She now has high-quality images that she can use to calculate the transmission matrix. The time required for the optimization procedure is 3 minutes and limited by the frame rate of the camera we used.

The security of the wavefront-shaping procedure is based on the same arguments as that of the security of the quantum communication after completion of the wavefront shaping: the no-cloning theorem forbids an attacker to fully characterize the light pulse containing fewer photons than the number of fiber modes and scrambled by the multimode fiber. Eve can record the light that is sent by Alice. However, since there is very little difference between the different phase masks (since there is less than photon in each segment), it is impossible for her to know what segment Alice is probing. Therefore, if Eve ‘replays’ the field to Bob’s fiber, she will just have to send some arbitrary wavefront. Now, when Alice sums Bob’s camera frames, she will not get a high-quality speckle image. Instead, she will get a completely washed-out noise pattern, which will signal the presence of the eavesdropper. Since Alice and Bob have not shared any secrets yet, no information leak is possible.

We have characterized the fidelity (efficiency) of the wavefront shaping by the parameter $\alpha^2 = P_f / P_0$, where P_f is the power in the focus area with a center corresponding to that of the focal spot and a diameter equal to the FWHM of the Gaussian spot. P_0 is the total power on the fiber output. We assume that any losses don’t influence the wavefront shaping quality but only the total signal. In the presented experiments, α^2 is 10%. In our experimental setup, the fidelity was limited by Eve’s interception part in the transmission line (see Figure 1). In practice, an uninterrupted fiber should be used. For such fibers, a fidelity close to $\pi/4$ was reported experimentally for phase-only wavefront shaping¹⁹.

Image processing

The signal was recorded by a HiCAM 5000 High-speed Intensified Camera (Lambert Instruments, the Netherlands) with 512x512 pixels and a speed of 5000 fps. To keep well-defined sensitivity, the incident photon flux is restricted to not exceed 5 detection events per frame on average. To investigate the parameters of secure communication with a higher number of photons, we summed up the required number of frames measured in the same conditions. As a result, an event with two or more photons at one point can be easily detected.

Information gained by Bob

We assume that Bob has S detectors, where $S < N$. The maximum amount of information that Bob can read out per received photon is $H_B = \log_2(S)$. In case of $S = 36$ symbols this maximum value is $H_B \approx 5.2$ bit of information. However, for a real-life situation, the fidelity of wavefront shaping will not be unity. The information Bob can gain per single photon detection event in this scenario can be calculated as

$$H_B \equiv H(B) - H(B|s), \quad (1)$$

where $H(B)$ is the entropy of the received alphabet, $H(B|s)$ the conditional entropy at the receiver side under the condition that symbol s was sent. We consider the situation when Bob takes into account only the symbols for which he got a click on one of the S detectors. The probability of getting a click on detector b in a case a random unknown symbol is sent, is

$$P(b) = \frac{1}{S}. \quad (2)$$

The total entropy, given that there was a click on one of the detectors is

$$H(B) = - \sum_{b=1}^S P(b) \log_2 P(b) = \log_2(S). \quad (3)$$

Now we calculate the conditional entropy $H(B|s)$, which is the amount of information that is needed to describe measurement outcome B given that the symbol s is known. The probability of getting a click on detector b given that symbol s was sent, is

$$P(b|s) = \begin{cases} \frac{\alpha^2}{\alpha^2 + \frac{1-\alpha^2}{N-1}(S-1)}, & \text{if } s = b \\ \frac{1-\alpha^2}{(N-1) \left[\alpha^2 + \frac{1-\alpha^2}{N-1}(S-1) \right]}, & \text{if } s \neq b \end{cases} \quad (4)$$

where N is the number of modes, S is the number of symbols, and α^2 is the fidelity of the wavefront shaping. As a result, the conditional entropy is

$$H(B|S) = -(S-1) P(b|s \neq b) \log_2(P(b|s \neq b)) - P(b|s = b) \log_2(P(b|s = b)). \quad (5)$$

Using equations (1), (3) and (5) we find that the information, which Bob can get per single photon detection in case of non-perfect wavefront shaping, is

$$H_B = \log_2(S) + (S-1) P(b|s \neq b) \log_2(P(b|s \neq b)) + P(b|s = b) \log_2(P(b|s = b)). \quad (6)$$

This value was used to analyse the parameters for which the amount of information per photon gained by Bob in imperfect conditions becomes more than the theoretically possible maximum of information gained by Eve.

Attacker model

We aim at proving security of our multimode-fiber-based method of communication. In particular, we give security bounds in the case where Eve's attack on the quantum channel is not restricted. We consider the following classification of attacker models, following Scarani *et al.*⁴

We analyze *individual attacks* and their essential subfamily, the *intercept-resend attacks*. As the name indicates, in this class of attacks, Eve intercepts the signal somewhere on its way from Alice to Bob, performs a measurement on it, and prepares a new signal that she sends to Bob (see Fig. 1). The part of the fiber controlled by Bob is inaccessible to Eve.

Collective attacks, which imply that Eve keeps data in a quantum memory until the end of the classical post processing, are, fortunately, not applicable for our method. The great advantage of our multimode-fiber-based method is that it doesn't require a quantum key sifting step or any other classical post processing. Eve would not benefit from storing all the intercepted light in a quantum memory during the calibration phase because 1) she will never find out how to combine them successfully (only Alice knows the order of the phase masks) and 2) her intercept attack would be detected, since Eve would be forced to send random wavefronts to Bob.

General attacks, includes many possible variations and cannot be efficiently parametrized. Nevertheless, bounds for unconditional security have been found in many cases and in all these cases, it turns out that the bound is the same as for collective attacks⁴.

Hacking attacks are related to the weaknesses of a practical implementation. The best-known example is the family of *Trojan horse attacks*, in which Eve probes the settings of Alice's and/or Bob's devices by sending some light into the system and register the reflected signal. However, in the setup

where light goes only one way, the solution against Trojan horse attacks consists in using an optical isolator⁴, which can be easily implemented in our setup.

Security analysis for a single-photon Fock state

We assume that Alice uses a perfect single-photon source to send symbols and Eve can read the signal somewhere in the middle of the fiber, potentially close to Alice or close to Bob. Additionally, since Alice sends a single photon, we assume that Eve performs intensity measurements. We now find a strict upper limit of information that can be gained by Eve by considering the hypothetical scenario (excluded by our calibration process) where Eve somehow knows the basis (what field arrives at pixel e of her detector when Alice sends a given symbol s), but is not able to build a passive linear-optical mode convertor to sort the intercepted photons efficiently into S detectors. Let's call this the field transmission function t_{es} . Neglecting losses and assuming Eve has a perfect detector (with N pixels, one for each mode in the fiber), she will get exactly one click on one pixel of her detector for each symbol that is sent. We are now interested in calculating how much information Eve obtains by recording this single photon. The maximum amount of information that Eve can get is

$$H_E \equiv H(E) - H(E|s). \quad (7)$$

Here, the entropy $H(E)$ is the amount of information that is needed to describe a measurement outcome E and the conditional entropy $H(E|s)$ is the amount of information that is needed to describe this outcome when it is known which symbol s was sent. By Bayes' rule for conditional entropy, the difference between the two entropies H_E is the maximum amount of information that Eve can possibly gain. We are now left with the task of calculating the conditional entropy given that the symbol s is known.

$$H(E|s) = - \sum_e^N P(e|s) \log_2 P(e|s), \quad (8)$$

with $P(e|s) \equiv |t_{es}|^2$ the probability for a photon sent as symbol s to arrive at pixel e . Since there are no losses, $\sum_e^N |t_{es}|^2 = 1$. The exact value of $H(E|s)$ depends on the unknown, random transmission matrix elements and, therefore, is impossible to predict in advance. However, we can readily find the ensemble averaged value $\langle H(E|s) \rangle$, i.e. the conditional entropy averaged over all possible random transmission matrices of the fiber. To do so, we assume that $\langle |t_{es}|^2 \rangle = 1/N$ and that the elements $|t_{es}|^2$ are drawn from independent exponential distributions. In the case of a large number of modes N , the distribution of $|t_{es}|^2$ equals $P(|t_{es}|^2) = N \exp(-|t_{es}|^2 N)$. To calculate the expected value for $H(E|s)$, we average over realizations of disorder. Substituting $y_{es} \equiv |t_{es}|^2 N$ we can write

$$\langle H(E|s) \rangle \equiv - \frac{1}{N} \sum_e^N \int_0^\infty \exp(-y_{es}) y_{es} \log_2(y_{es}/N) dy_{es}. \quad (9)$$

Since the distribution of y does not depend on s or e , we can omit averaging over all symbols

$$\langle H(E|s) \rangle = - \int_0^\infty \exp(-y) y (\log_2 y - \log_2 N) dy = \log_2 N - \int_0^\infty \exp(-y) y \log_2 y dy. \quad (10)$$

This integral evaluates to

$$\langle H(E|s) \rangle = \log_2 N - \frac{1 - \gamma}{\ln 2}, \quad (11)$$

with the Euler constant $\gamma \approx 0.577216$. Using (1) we finally find

$$\langle H_E \rangle = \frac{1 - \gamma}{\ln 2} \approx 0.61 \text{ bit.} \quad (12)$$

Hence, Eve gains only 0.61 bit of information per transmitted symbol at best, regardless of the number of symbols or modes even in the extreme case when she knows the exact basis. Under the same conditions, Bob will have at maximum $H_B(S) = \log_2(S) \approx 5.2$ bit of information per transmitted symbol for 36 symbols. As a result, $\langle H_E \rangle \ll H_B$, guaranteeing the security of the method.

Security analysis for coherent state

We assume that Eve is somehow able to record the field in each of the fiber modes independently, e.g. by a homodyning technique. The accuracy of these measurements will be limited by shot noise in the reference. When Alice sends a symbol s with field amplitude μ , at Eve's side the field in mode e equals $E_e = \mu t_{es}$. However, due to shot noise, Eve will actually measure $(\mathbf{E}_{\text{Eve}})_e = \mu t_{es} + \xi_e$, with ξ_e a noise term with $\bar{\xi}_e = 0$ and $|\bar{\xi}_e|^2 = 1$ photon, where $\bar{\cdot}$ indicates averaging over measurements²⁵.

We now proceed to calculate the amount of information that Eve gains by doing this measurement. Eve can first project her measurement of the field at the fiber output \mathbf{E}_{Eve} on the basis of symbols by simply multiplying with t_{es}^{-1} . When all modes of the fiber are used ($S = N$) and the fiber is lossless, t_{es} is unitary. After performing the transformation, Eve will have found the vector $\mathbf{E} \equiv t_{es}^{-1} \mathbf{E}_{\text{Eve}}$, where each element in \mathbf{E} corresponds to a symbol. Averaged over measurements we find $\bar{\mathbf{E}} = \mu_s$, where μ_s is a vector with a value of μ at index s , and zero everywhere else. Importantly, since the transformation is unitary and the noise in different components of \mathbf{E}_{Eve} is uncorrelated, the transformation does not alter the noise statistics of the elements of \mathbf{E} : i.e. the noise term has a complex Gaussian distribution with $|\bar{\xi}_e|^2 = 1$ photon. When $S < N$, it is still possible to define a unitary matrix t_{es} that maps all possible symbols to the first S indices of E and maps all unused state to the remaining indexes. Eve can simply discard the values at these remaining indices since they will never contain any information. Therefore, below we consider \mathbf{E} to be a vector of length S .

When Alice sends symbol s , the transformed vector \mathbf{E} is drawn from the probability density function

$$P(\mathbf{E}|s) = \frac{e^{-\|\mathbf{E} - \mu_s\|^2}}{\pi^S}. \quad (13)$$

The differential entropy of this complex multivariate normal distribution is given by $H(E|s) = S \log_2 \pi + S/\ln(2)$. We need to compare this value to the entropy for the case that it is not known what symbol was sent. In this case, the probability density equals

$$P(\mathbf{E}) = \frac{1}{S} \sum_{s=1}^S \frac{e^{-\|\mathbf{E} - \mu_s\|^2}}{\pi^S}. \quad (14)$$

Unfortunately, there is no known closed form expression for the entropy of such a Gaussian mixture³¹. Therefore, we use a Monte Carlo approach to calculate the entropy of (8) numerically (see Figure 3(a)). Additionally, it is straightforward to derive an upper limit for the entropy. First, we realize that the real parts of the components of \mathbf{E} all have a mean value of μ/S and a variance of $\frac{1}{2} + \frac{(S-1)}{S} \left(\frac{\mu}{S}\right)^2 + \frac{1}{S} \left(\mu - \frac{\mu}{S}\right)^2 = \frac{1}{2} + \frac{\mu^2(S-1)}{S^2}$. The imaginary parts have a mean of 0 and a variance of 1/2. The maximum entropy distribution for a given variance is Gaussian. Therefore, our distribution (see equation (14)) must have a lower entropy than a Gaussian with the same variance. The differential entropy for this Gaussian is simply given by $H(\mathbf{E})_{\text{upper}} = \frac{1}{2} \log_2(|2\pi e \Sigma|) = S \log_2 \pi + S/\ln(2) + (S/2) \log_2(1 +$

$2\mu^2(S - 1)/S^2$) with Σ the covariance matrix, which is diagonal in our case. Half of the diagonal elements are $\frac{1}{2} + \mu^2(S - 1)/S^2$ (for the real parts), the rest (for the imaginary parts) is $\frac{1}{2}$, so $|2\pi e\Sigma| = (\pi e)^S (\pi e(1 + 2\mu^2(S - 1)S^{-2}))^S$. The upper limit for the entropy gained by Eve follows by subtracting $H(E|s)$, and also realizing that Eve cannot collect more information than what is being sent by Alice.

$$H_E < \min \left[\frac{S}{2} \log_2 \left(1 + 2\mu^2 \frac{S-1}{S^2} \right), \log_2 S \right]. \quad (15)$$

As long as, $H_E < H_B$ the method remains secure even in the extreme case of a weak coherent light source with more than 1 photon per pulse in a non-secret basis.

Security analysis for calibration phase

During the calibration phase, Alice changes the phase of a single segment of the light modulator, meaning that the wavefront is largely plane. We can describe this wave as a superposition of a plane wave and a part corresponding to the modulated segment. Since the intensity is distributed equally over all N_{seg} segments, the value of μ as used in the analysis above would be $\mu = \bar{n}_c/N_{seg}$, with \bar{n}_c the average number of photons sent during a single pulse in the calibration measurement (in our case, amounting to $\mu = (80 \pm 30)/1156$ photons). As can be seen from the analysis above, from this measurement Eve cannot determine what symbol was sent with any reasonable confidence, so she cannot intercept the calibration phase. Note that the plane-wave component of the wavefront contains much more energy. However, this component does not carry any information, so Eve does not gain anything by intercepting it.

DATA AVAILABILITY

The data that support the findings of this study are available from the corresponding authors upon request.

ACKNOWLEDGEMENTS

We thank Klaus Boller, Ad Lagendijk, Mehul Malik, Ravi Uppu, and Willem Vos for discussions and acknowledge funding by a Vici grant from the Netherlands Organisation for Scientific Research (NWO). IMV acknowledges funding from ERC Starting grant n° 678919. LVA acknowledges funding from NWO VENI grant (15872).

CONFLICT OF INTERESTS

We have no conflict of interest to declare.

REFERENCES

1. Lo, H.-K., Curty, M. & Tamaki, K. Secure quantum key distribution. *Nat. Photonics* **8**, 595–604 (2014).
2. Rivest, R. L., Shamir, A. & Adleman, L. A method for obtaining digital signatures and public-key cryptosystems. *Commun. ACM* **21**, 120–126 (1978).
3. Wootters, W. K. & Zurek, W. H. A single quantum cannot be cloned. *Nature* **299**, 802–803 (1982).

4. Scarani, V. *et al.* The security of practical quantum key distribution. *Rev. Mod. Phys.* **81**, 1301–1350 (2009).
5. Bennett, C. H. & Brassard, G. Quantum cryptography : Public key distribution and coin tossing. *Int. Conf. Comput. Syst. Signal Process. IEEE 1984* 175–179 (1984).
6. Proakis, J. G. *Wiley Encyclopedia of Telecommunications*. (Wiley-Interscience, 2003).
7. Richardson, D. J., Fini, J. M. & Nelson, L. E. Space-division multiplexing in optical fibres. *Nat. Photonics* **7**, 354–362 (2013).
8. Ding, Y. *et al.* High-dimensional quantum key distribution based on multicore fiber using silicon photonic integrated circuits. *Npj Quantum Inf.* **3**, 25 (2017).
9. Bromberg, Y. *et al.* Remote key establishment by random mode mixing in multimode fibers and optical reciprocity. *Opt. Eng.* **58**, 016105 (2019).
10. Plöschner, M., Tyc, T. & Čížmár, T. Seeing through chaos in multimode fibres. *Nat. Photonics* **9**, 529–535 (2015).
11. Gloge, D. Optical Power Flow in Multimode Fibers. *Bell Syst. Tech. J.* **51**, 1767–1783 (1972).
12. Snyder, A. W. & Love, J. D. *Optical waveguide theory*. (Chapman and Hall, 1983).
13. Vellekoop, I. M. & Mosk, A. P. Focusing coherent light through opaque strongly scattering media. *Opt. Lett.* **32**, 2309–2311 (2007).
14. Vellekoop, I. M., Lagendijk, A. & Mosk, A. P. Exploiting disorder for perfect focusing. *Nat. Photonics* **4**, 320–322 (2010).
15. Jang, J. *et al.* Complex wavefront shaping for optimal depth-selective focusing in optical coherence tomography. *Opt. Express* **21**, 2890 (2013).
16. Amitonova, L. V., Mosk, A. P. & Pinkse, P. W. H. Rotational memory effect of a multimode fiber. *Opt. Express* **23**, 20569–20575 (2015).
17. Amitonova, L. V. *et al.* High-resolution wavefront shaping with a photonic crystal fiber for multimode fiber imaging. *Opt. Lett.* **41**, 497 (2016).
18. Descloux, A., Amitonova, L. V. & Pinkse, P. W. Aberrations of the point spread function of a multimode fiber due to partial mode excitation. *Opt. Express* **24**, 18501–18512 (2016).

19. Čižmár, T. & Dholakia, K. Shaping the light transmission through a multimode optical fibre: complex transformation analysis and applications in biophotonics. *Opt. Express* **19**, 18871–18884 (2011).
20. Čižmár, T. & Dholakia, K. Exploiting multimode waveguides for pure fibre-based imaging. *Nat. Commun.* **3**, 1027 (2012).
21. Di Leonardo, R. & Bianchi, S. Hologram transmission through multi-mode optical fibers. *Opt. Express* **19**, 247–254 (2011).
22. Vellekoop, I. M. Feedback-based wavefront shaping. *Opt. Express* **23**, 12189 (2015).
23. Vellekoop, I. M. & Mosk, A. P. Universal Optimal Transmission of Light Through Disordered Materials. *Phys. Rev. Lett.* **101**, (2008).
24. Gisin, N., Ribordy, G., Tittel, W. & Zbinden, H. Quantum cryptography. *Rev. Mod. Phys.* **74**, 145 (2002).
25. Jang, M., Yang, C. & Vellekoop, I. M. Optical Phase Conjugation with Less Than a Photon per Degree of Freedom. *Phys. Rev. Lett.* **118**, (2017).
26. Hu, J.-Y. *et al.* Experimental quantum secure direct communication with single photons. *Light Sci. Appl.* **5**, e16144 (2016).
27. Carolan, J. *et al.* Universal linear optics. *Science* **349**, 711–716 (2015).
28. Labroille, G. *et al.* Characterization and applications of spatial mode multiplexers based on Multi-Plane Light Conversion. *Opt. Fiber Technol.* **35**, 93–99 (2017).
29. Tentrup, T. B. H. *et al.* Transmitting more than 10 bit with a single photon. *Opt. Express* **25**, 2826–2833 (2017).
30. Conkey, D. B., Caravaca-Aguirre, A. M. & Piestun, R. High-speed scattering medium characterization with application to focusing light through turbid media. *Opt. Express* **20**, 1733–1740 (2012).
31. Kim, S. M., Do, T. T., Oechtering, T. J. & Peters, G. On the Entropy Computation of Large Complex Gaussian Mixture Distributions. *IEEE Trans. Signal Process.* **63**, 4710–4723 (2015).

FIGURES

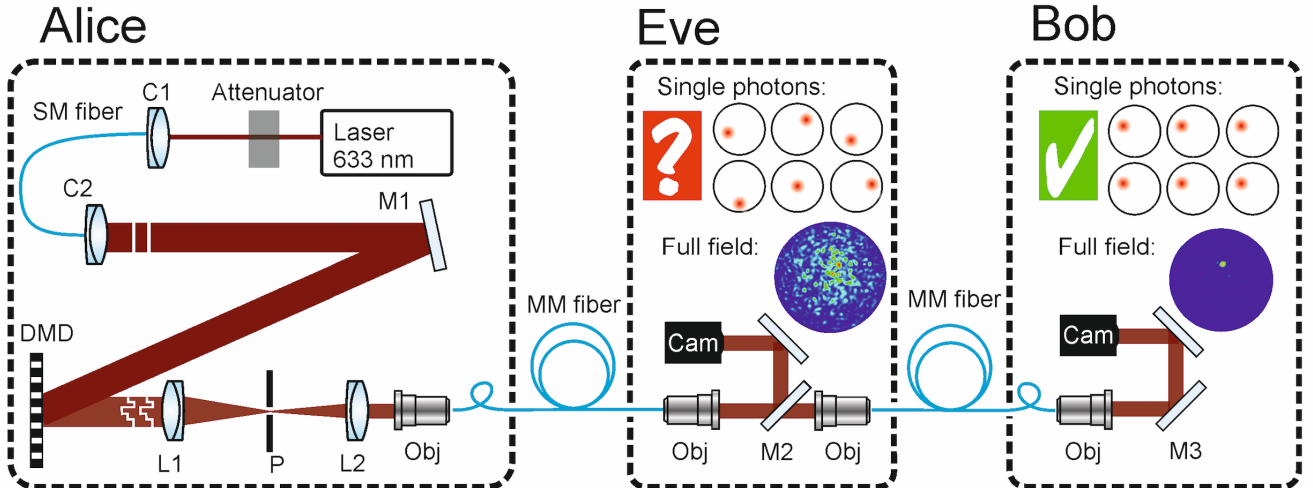


Figure 1. Experimental setup. Alice encodes a symbol by coupling light with an appropriate phase pattern into a multimode fiber. Bob receives a signal focused at a particular position on the fiber output facet (see ‘Full field’ on Bob’s part). Bob can reconstruct the position even with a single detected photon (see ‘Single photons’ on Bob’s part). With mirror M2 Eve can tap off the signal in the middle of the fiber. However, due to the mode-mixing nature of the multimode fiber, her intensity distribution is a complex interference pattern (see ‘Full field’ on Eve’s part). The positions of her photon detections are random and vary even for different realizations of the same symbol (see ‘Single photons’ on Eve’s part). As a result, Eve cannot reconstruct the symbol that Alice sent. Abbreviations: MM fiber, multimode fiber; DMD, digital micromirror device; SM fiber, single mode fiber; M, mirror; L, lens; Obj, objective; P, pinhole; C, collimator; Cam, camera.

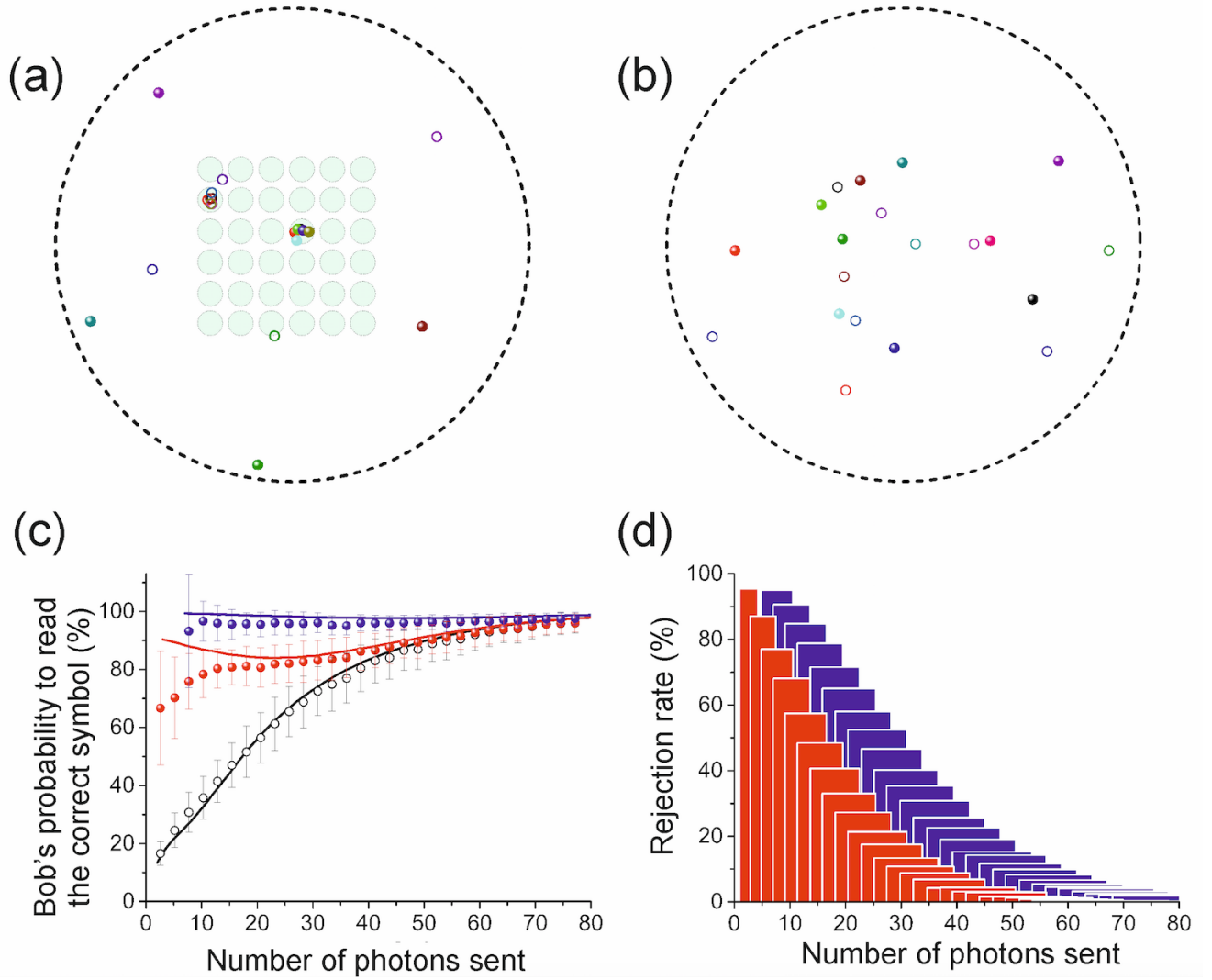


Figure 2. Experimental demonstration of secure communication. **a, b.** Snapshots of the spatial distributions of photons measured by Bob (a) and by Eve (b) in case of a perfect single-photon source and a fidelity of wavefront shaping $\alpha^2 = 0.6$. The open and filled dots correspond to two different symbols sent by Alice. Different colors represent 10 different repetitions of each of the symbols. The dashed line indicates the fiber core edge. Faint green circles on Bob's facet represent the symbol areas. In contrast to the photon distribution measured by Eve, Bob clearly sees the correlation between different realizations of the same symbol. **c.** The measured probability of Bob to detect the correct symbol versus the average number of photons in a pulse for wavefront shaping fidelity $\alpha^2 = 0.1$, a weak coherent light source and different strategies: Bob uses no threshold (black); Bob accepts only symbols that have been triggered by two or more photons (red) and three or more photons (blue). Vertical error bars represent the standard deviation after averaging over 36 symbols. Solid lines show the theoretical calculations of the probabilities as described in the main text. **d.** The rejection ratio for a threshold of 2 photons (red bars) and 3 photons (blue bars) versus the average number of detected photons in a pulse. The width of the bars corresponds to the standard deviations of the number of photons in a pulse and increases according to a Poisson distribution.

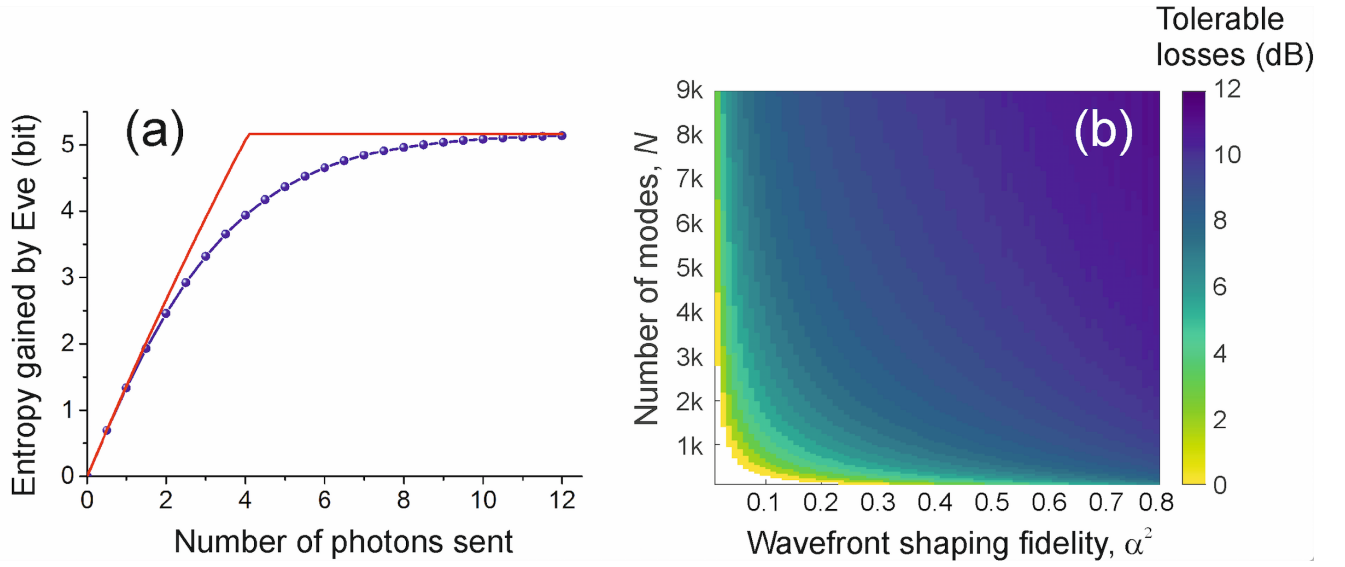


Figure 3. Security analysis for weak coherent light source. **a.** Entropy per transmitted symbol gained by Eve for $N = 1500$ fiber modes and $S = 36$ symbols. The connected blue dots represent the exact entropy function (evaluated through a numerical integration method) and the red line is a closed form expression that gives a simple upper limit (see Methods section). The result is independent of the wavefront shaping fidelity. **b.** The maximum level of losses in dB for our method to be secure for a weak coherent light source as a function of wavefront shaping fidelity, α^2 and the number of modes N , for an alphabet consisting of $S = 36$ symbols.